The crystal and magnetic structure of the magnetocaloric compound $FeMnP_{0.5}Si_{0.5}$

Viktor Höglin [a,*], Matthias Hudl [b], Martin Sahlberg [a], Per Nordblad [b], Premysl Beran [c], Yvonne Andersson [a]

[a] *Department of Materials Chemistry, Uppsala University, Box 538, 75121 Uppsala, Sweden*
[b] *Department of Engineering Sciences, Uppsala University, Box 534, 75121 Uppsala, Sweden*
[c] *Nuclear Physics Institute, Academy of Sciences of the Czech Republic, 25068 Rez, Czech Republic*

ABSTRACT

The crystal and magnetic structure of the magnetocaloric compound $FeMnP_{0.5}Si_{0.5}$ has been studied by means of neutron and X-ray powder diffraction. Single phase samples of nominal composition $FeMnP_{0.5}Si_{0.5}$ have been prepared by the drop synthesis method. The compound crystallizes in the Fe_2P-type structure ($P\bar{6}2m$) with the magnetic moments aligned along the a-axis. It is found that the Fe atoms are mainly situated in the tetrahedral 3g site while the Mn atoms prefer the pyramidal 3f position. The material is ferromagnetic ($T_C=382$ K) and at 296 K the total magnetic moment is 4.4 μ_B/f.u. It is shown that the magnetic moment in the 3f site is larger (2.5 μ_B) than in the 3g site (1.9 μ_B).

© 2011 Elsevier Inc. All rights reserved.

1. Introduction

Magnetocaloric compounds have gained an increased interest since the middle 1990s due to environmental and energy benefits from magnetic refrigeration and the discovery of the giant magnetocaloric effect (GMCE) [1]. In GMCE compounds rare earth metals are common alloying elements and due to their rareness in nature and high costs, they will be a problem in a future large-scale production. Hence, there is a need to find more common and cheaper compounds not based on rare earth metals that possess the GMCE.

A large number of studies on the compound Fe_2P have been performed since the 1960s and its crystallographic and magnetic properties have been well investigated [2–4]. The relatively large saturation magnetization, first order nature of the transition and readily tunable transition temperature with various substitutions make the Fe_2P system a candidate compound for magnetocaloric applications. Numerous compounds based on Fe_2P have been fabricated during the years and compounds of the $FeMnP_{1-x}M_x$-type (M=Si, Ge and/or As) have shown improved magnetocaloric properties.

In this investigation, samples of nominal composition $FeMnP_{0.5}Si_{0.5}$ have been synthesized and the crystal and magnetic structure and the magnitude of the magnetic moments at different temperatures have been determined. There is a controversy about the exact properties of the $FeMnP_{1-x}Si_x$-system. A previous study by Cam Thanh et al. [5] on samples of nominally the same composition, $FeMnP_{0.5}Si_{0.5}$, prepared by a ball milling technique, had a transition temperature of 332 K with higher preserved magnetocaloric effect. There is a significant difference in the structural and magnetic properties presented by Cam Thanh et al. [5] compared to our results. This dichotomy may be explained by the fact that their samples contained about 18% of a second phase, identified as Fe_2MnSi.

Our magnetization measurements on the $FeMnP_{0.5}Si_{0.5}$ sample show a ferromagnetic transition temperature of 382 K and the magnetic entropy change $-\Delta S_M$ from magnetization experiments has been estimated to about 8 J/kgK in a magnetic field change of 1.8 T [6]. The magnetocaloric effect is slightly lower compared to similar compounds [7,8] but due to its content of only common, non-toxic, elements $FeMnP_{0.5}Si_{0.5}$ is a promising magnetocaloric compound within the $FeMnP_{1-x}M_x$ alloy system.

2. Experiments

2.1. Sample preparation

$FeMnP_{0.5}Si_{0.5}$ samples were prepared by the drop synthesis method [9] using a high frequency induction furnace at 1623–1673 K in an Ar atmosphere of 40 kPa. Stoichiometric

---

amounts of iron (Leico Industries, purity 99.995%. Surface oxides were reduced in H_2-gas.), manganese (Institute of Physics, Polish Academy of Sciences, purity 99.999%), phosphorus (Cerac, purity 99.999%) and silicon (Highways International, purity 99.999%) were used as raw materials. All samples were crushed, pressed into pellets and sealed in evacuated fused silica tubes. Subsequently, the samples were sintered at 1373 K for 1 h, annealed at 1073 K for 65 h and finally quenched in cold water.

2.2. X-ray powder diffraction

Phase analysis and crystal structure characterizations were performed using X-ray powder diffraction (XRD) with a Bruker D8 diffractometer equipped with a Våntec position sensitive detector (PSD, 4° opening) using Cu$K\alpha_1$ radiation, $\lambda = 1.540598$ Å. The measurements were made using a 2θ-range of 20–90° at 296 and 403 K and a 2θ-range of 35–60° in the temperature range 373–393 K.

2.3. Neutron powder diffraction

Neutron powder diffraction data were collected on the instrument MEREDIT at the Nuclear Physics Institute in Rez, Czech Republic. The neutron beam was monochromatized by a copper mosaic monochromator (reflection 220) giving a wavelength of $\lambda = 1.46$ Å. Samples were studied in a 2θ-range of 4–148° at 296 and 450 K.

2.4. Refinements of the crystal and magnetic structure

Structure refinements were performed on the neutron powder profiles by the Rietveld method [10] using the software FULLPROF [11] and unit cell parameters from XRD data were refined using the software UNITCELL [12]. The neutron wavelength was refined by using unit cell parameters determined from XRD data as starting point. The refined wavelength was used to refine the unit cell parameters at 450 K from neutron powder diffraction data. The peak shape was described by a pseudo-Voight profile function and the background was determined by a linear interpolation between chosen points. The following parameters in the 450 K dataset were varied: peak shape, unit cell parameters, scale factor, half width parameters, zero point, background, atom occupancies, isotropic temperature parameter and atomic coordinates. The same parameters of the 296 K dataset were varied as well as the parameters for the magnetic moments. The magnetic form factors of Fe and Mn were set as
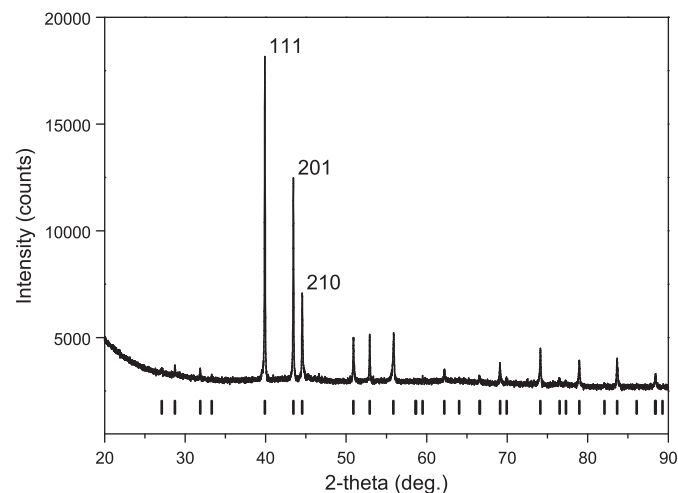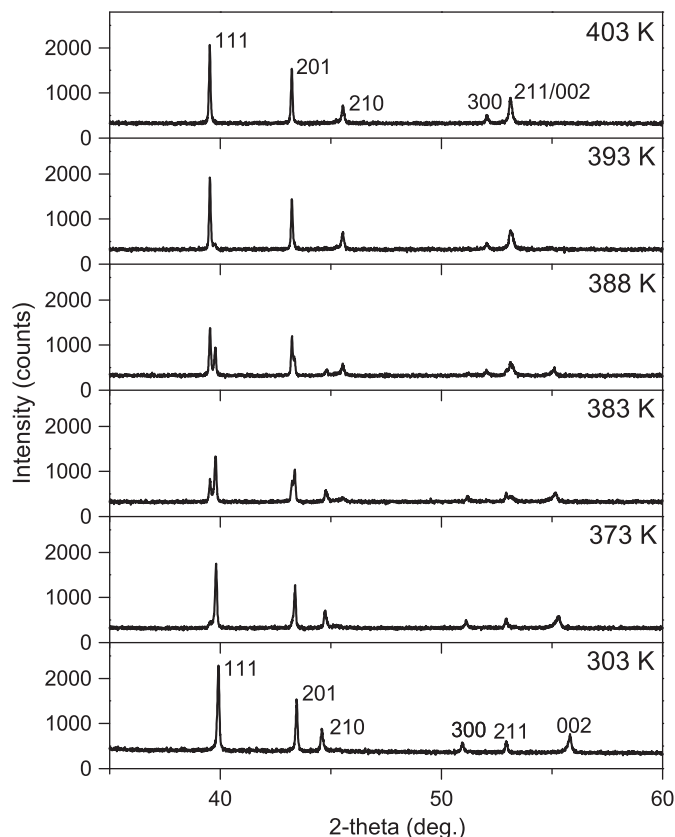

Fig. 2. XRD-patterns of FeMnP$_{0.5}$Si$_{0.5}$ showing the structural transition occurring at approx. 385 K. $\lambda = 1.540598$ Å.

Table 1
Unit cell parameters of FeMnP$_{0.5}$Si$_{0.5}$ at 296 and 450 K refined from XRD data, $\lambda = 1.540598$ Å.

T (K)	a (Å)	c (Å)	V (Å³)	c/a
296	6.2090(3)	3.2880(2)	109.78(2)	0.5296(1)
450	6.0830(8)	3.4507(9)	110.58(4)	0.5672(1)

Fig. 1. X-ray powder diffraction pattern of FeMnP$_{0.5}$Si$_{0.5}$ at 296 K. The tick marks indicate the Bragg positions of FeMnP$_{0.5}$Si$_{0.5}$. $\lambda = 1.540598$ Å.

Table 2
Interatomic distances in FeMnP$_{0.5}$Si$_{0.5}$ at 296 K.

Atoms	Distance (Å)
Fe(1)	
2 P/Si(2)	2.292(2)
2 P/Si(1)	2.342(2)
2 Mn(2)	2.675(5)
4 Mn(2)	2.742(1)
2 Fe(1)	2.766(3)
P/Si(1)	
3 Fe(1)	2.342(2)
6 Mn(2)	2.506(5)
Mn(2)	
1 P/Si(2)	2.502(6)
4 P/Si(1)	2.506(2)
2 Fe(1)	2.675(5)
4 Fe(1)	2.742(4)
4 Mn(2)	3.275(6)
P/Si(2)	
6 Fe(1)	2.292(2)
3 Mn(2)	2.502(3)

Table 3
Placement and occupancy of the Fe and Mn atoms in $FeMnP_{0.5}Si_{0.5}$ at 296 and 450 K. Derived from refinements of neutron powder diffraction data. (0,0,0) was chosen as an origin.

Atom	Site	296 K				450 K			
		x	y	z	Occ.	x	y	z	Occ.
Fe(1)	3g	0.2572(4)	0	1/2	0.2353(4)	0.2548(3)	0	1/2	0.2353(4)
Mn(1)	3g	0.2572(4)	0	1/2	0.0147(4)	0.2548(3)	0	1/2	0.0147(4)
Fe(2)	3f	0.597(1)	0	0	0.0193(2)	0.591(1)	0	0	0.0193(2)
Mn(2)	3f	0.597(1)	0	0	0.2307(2)	0.591(1)	0	0	0.2307(2)
P/Si(1)	2d	1/3	2/3	1/2	0.1667	1/3	2/3	1/2	0.1667
P/Si(2)	1a	0	0	0	0.0833	0	0	0	0.0833
		$R_p=2.37\%$, $R_{wp}=3.05\%$, $\chi^2=3.03$				$R_p=2.59\%$, $R_{wp}=3.36\%$, $\chi^2=3.44$			
		$R_{Bragg}=5.26\%$, $R_{mag}=6.08\%$				$R_{Bragg}=4.53\%$			

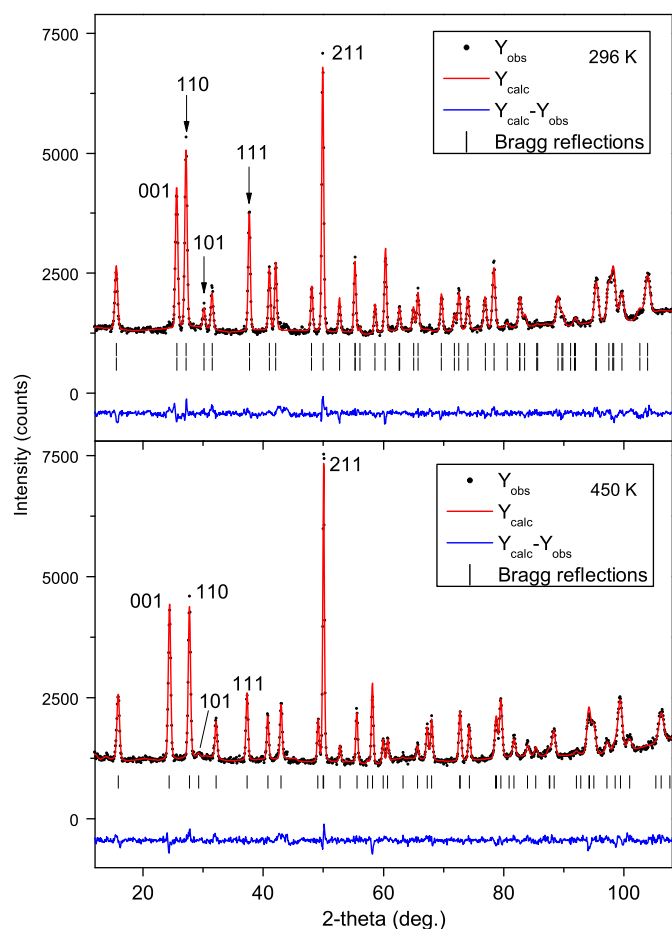**Fig. 3.** Structure refinements from neutron powder diffraction data of $FeMnP_{0.5}Si_{0.5}$ at 296 and 450 K. The differences in intensity and position of the Bragg peaks are due to the ferro- to paramagnetic transition at ∼ 390 K and the structural transition at ∼ 385 K. The peaks with the highest magnetic intensity are marked with an arrow.

shown in Refs. [13,14], respectively. The occupancies of the P/Si sites were kept at a 50/50 ratio, thus not allowing the actual P and Si content to be determined from these refinements.

3. Results

3.1. Phase analysis and crystal structure

The XRD investigation confirms that $FeMnP_{0.5}Si_{0.5}$ crystallizes in the hexagonal Fe_2P-type structure, space group $P\bar{6}2m$ and unit cell parameters $a=6.2090(3)$ Å, $c=3.2880(3)$ Å. The XRD pattern for
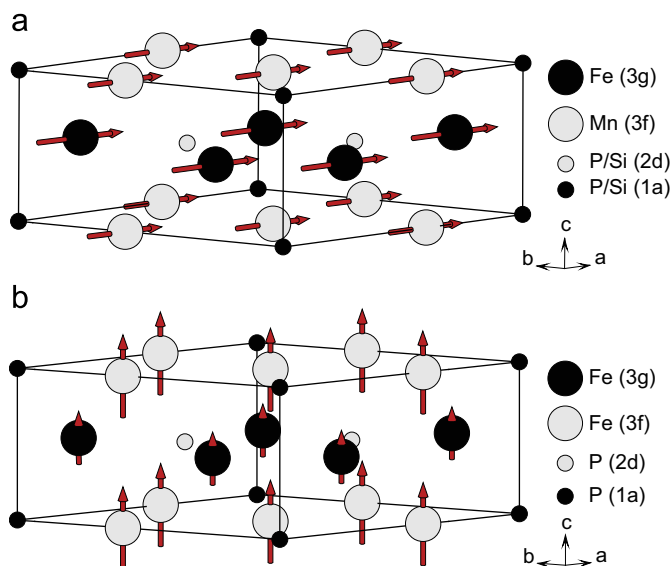

Fig. 4. The magnetic structure of $FeMnP_{0.5}Si_{0.5}$ (a) and Fe_2P (b). The magnetic moments in Fe_2P are aligned in the c-direction while the moments in $FeMnP_{0.5}Si_{0.5}$ are aligned in the a-direction. The length of the arrows corresponds to the magnitude of the magnetic moments.

$FeMnP_{0.5}Si_{0.5}$ at 296 K is shown in Fig. 1 which reveals a pattern of a single phase sample. XRD-patterns in the range 363–403 K are shown in Fig. 2 where it can be seen that $FeMnP_{0.5}Si_{0.5}$ undergoes a structural transition (within the space group) between ∼ 373 and 393 K. The a-axis has decreased ∼ 2% while the c-axis has increased ∼ 5% compared to 296 K, see Table 1. The factor c/a and the volume have increased ∼ 7% and 1%, respectively. The structural transition occurs in the same region as the Curie temperature why it is likely that the transition originate from magnetostriction effects. Structure refinements of powder neutron diffraction data show that the Fe and Mn atoms are preferably situated in the 3g and 3f sites, respectively, which are based on the interatomic distances (see Table 2) and the refined occupancies of the Fe and Mn atoms (see Table 3).

The composition based on the refined occupancies extracted from the neutron powder diffraction data (at fixed ratio P/Si=1) indicates that the acquired composition of the metallic atoms in the sample is close to $FeMnP_{0.5}Si_{0.5}$ ($Fe_{1.02(1)}Mn_{0.98(1)}P_{0.5}Si_{0.5}$, namely). Also, the synthetic process with stoichiometric amounts of the raw materials showed minor (less than 0.5%) losses.

3.2. Magnetic structure

Refinements of the neutron powder diffraction data at 296 and 450 K are shown in Fig. 3. The magnetic contribution from the

Table 4
Magnetic state, Fe saturation magnetic moment and interatomic average distances for tetrahedral Fe_t in FeMX with Fe_2P-structure, M_p=pyramidal Fe or Mn and X=P, Si and As.

Compound	Magn. state (T_C)	Fe_t sat. mom. (μ_B)	V (Å^3)	Fe_t–X (Å)	Fe_t–Fe_t (Å)	Fe_t–M_p (Å)	Reference
Fe_2P	PM (295 K)	–	103.1	2.255	2.610	2.682	[9]
	FM (77 K)	1.03	102.9	2.253	2.597	2.682	[15]
$FeMnP_{0.7}As_{0.3}$	PM (250 K)	–	110.7	2.311	2.638	2.755	[16]
	FM (100 K)	1.25	110.2	2.312	2.747	2.743	[16]
$FeMnP_{0.5}Si_{0.5}$	PM (450 K)	–	109.8	2.312	2.685	2.726	This work
	FM (296 K)	1.65	110.6	2.317	2.766	2.708	This work

ferromagnetic phase at 296 K is distinguished by the higher peak-intensities at lower 2θ-angles. The magnetic moments are aligned in the a-direction and are 1.9(1) μ_B and 2.5(1) μ_B in the M(1) and M(2) site, respectively, which gives a total magnetic moment of 4.4(2) μ_B. The magnetic symmetry group was found to be $Cm2m$ with the magnetic unit cell $a=a_{hex}$, $b=\sqrt{3}a_{hex}$, $c=c_{hex}$ and $\alpha,\beta,\gamma = 90°$ where a_{hex} and c_{hex} are the unit cell parameters of the hexagonal Fe_2P-structure of $FeMnP_{0.5}Si_{0.5}$, see Table 1.

4. Discussion

The magnitude of the magnetic moments of the Fe atoms and the total magnetic moment per formula unit is confirmed by recent Mössbauer and magnetization studies of $FeMnP_{0.5}Si_{0.5}$ [6]. The total magnetic moment has been reported to be approx. 4.4 μ_B/f.u. which is in good agreement with our result, where the total magnetic moment is 4.4(2) μ_B/f.u. The size of the total magnetic moment is higher than the corresponding value for Fe_2P (2.9(1) μ_B) [17,18,15,19]. Earlier studies have also shown that there are significant differences in magnitude of the moments between the two Fe sites in Fe_2P. The Fe atom in the pyramidal 3f site possesses a smaller magnetic moment than the Fe atom in the tetrahedral 3g site, which is illustrated in Fig. 4(b).

The refinements of the neutron powder diffraction intensities of $FeMnP_{0.5}Si_{0.5}$ indicate that the Mn atoms prefer to be situated in the pyramidal 3f site in the Fe_2P-structure. The substitution of Fe with Mn in the 3f site increases the magnetic moment in the site by ~0.8 μ_B compared to Fe_2P. The magnetic moment of the Fe atom in the 3g site of $FeMnP_{0.5}Si_{0.5}$ is also shown to increase ~0.6 μ_B.

The magnetic structures of $FeMnP_{0.5}Si_{0.5}$ and Fe_2P are shown in Fig. 4. The magnetic moments are aligned in the a-direction while the moments of Fe_2P are aligned in the c-direction [4,20]. A similar alignment of the magnetic moments as in $FeMnP_{0.5}Si_{0.5}$ has also been reported to occur in $FeMnP_{0.5}As_{0.5}$ [16]. It is of interest to note that in $FeMnP_{0.7}As_{0.3}$ the moments deviate from the c-axis by 50°.

Magnetoelastic transitions have been found for the hexagonal system $FeMnP_{1-y}As_y$ ($0.15 \leq y \leq 0.66$) isostructural with $FeMnP_{0.5}Si_{0.5}$. A marked increase both in magnetic hyperfine field and in magnetic moment take place on the Fe tetrahedral site (Fe_t) as compared to the tetrahedral site in Fe_2P [16,21]. Table 4 displays the interatomic distances in paramagnetic and ferromagnetic Fe_2P, $FeMnP_{0.7}As_{0.3}$ and the presently studied compound $FeMnP_{0.5}Si_{0.5}$.

As can be seen from the table the cell volume, the average near Fe_t–X distances and Fe_t–M_p do not change significantly between the paramagnetic (PM) and the ferromagnetic (FM) state. However, the crystal a- and c-axes decrease and increase, respectively, when passing the first order ferromagnetic transition from lower

temperature. A large interatomic difference is, however, observed for the Fe_t–Fe_t distances for the high moment cases of $FeMnP_{0.7}As_{0.3}$ and $FeMnP_{0.5}Si_{0.5}$. The cell volume expansion between the three different compounds is obvious. The overall crystal expansion and the increase in Fe_t–Fe_t distances yield a stronger Fe_t electron localization and results in a larger Fe_t magnetic moment.

5. Conclusions

The magnetocaloric compound $FeMnP_{0.5}Si_{0.5}$ has been synthesized and studied regarding the crystallographic and magnetic structure. X-ray and neutron powder diffraction experiments show that the sample is single phase and reveals the magnetic structure of $FeMnP_{0.5}Si_{0.5}$. An isostructural phase transition has been observed at about the same temperature as the magnetic phase transition (382 K). The Fe atoms are mainly situated in the tetrahedral 3g site while the Mn atoms prefer the pyramidal 3f position. The magnetic moments derived from neutron powder diffraction are shown to be coordinated along the a-axis with a total moment of 4.4 μ_B. This high value of the magnetic moment goes along with our Mössbauer results [6] and is in accord with a strong increase in the Fe_t–Fe_t distances. The high magnetic moment and a readily tunable transition temperature make (slightly) off-stoichiometric $FeMnP_{0.5}Si_{0.5}$ a promising alloy system for magnetocaloric applications.

References

[1] V.K. Pecharsky, J.K.A. Gschneidner, Phys. Rev. Lett. 78 (1997) 4494.
[2] S. Rundqvist, F. Jellinek, Acta Chem. Scand. 13 (1959) 425.
[3] R. Wäppling, L. Häggström, S. Rundqvist, E. Karlsson, J. Solid State Chem. 3 (1971) 276.
[4] L. Lundgren, G. Tarmohamed, O. Beckman, B. Carlsson, S. Rundqvist, Phys. Scr. 17 (1978) 39.
[5] D.T. Cam Thanh, E. Brück, N.T. Trung, J.C.P. Klaasse, K.H.J. Buschow, Z.Q. Ou, O. Tegus, L. Caron, J. Appl. Phys. 103 (2008) 07B318.
[6] M. Hudl, L. Häggström, E.-K. Delczeg-Czirjak, V. Höglin, M. Sahlberg, P. Nordblad, L. Vitos, O. Eriksson, Y. Andersson, ⟨arXiv:1102.0636v1⟩, 2011.
[7] E. Brück, O. Tegus, L. Zhang, X.W. Li, F.R. de Boer, K.H.J. Buschow, J. Alloys Compd. 383 (2004) 32.
[8] D.T. Cam Thanh, E. Brück, O. Tegus, J.C.P. Klaasse, T.J. Gortenmulder, K.H.J. Buschow, J. Appl. Phys. 99 (2006) 08Q107.
[9] B. Carlsson, M. Gölin, S. Rundqvist, J. Solid State Chem. 8 (1973) 57.
[10] H.M. Rietveld, J. Appl. Crystallogr. 2 (1969) 65.
[11] J. Rodriguez-Carvajal, Fullprof.2k computer program, version 4.70, 2009.
[12] T. Holland, S. Redfern, Unitcell computer program, version 1, 2000.
[13] H. Fujii, S. Komura, T. Takeda, T. Okamoto, Y. Ito, J. Akimitsu, J. Phys. Soc. Jpn. 46 (1979) 1616.
[14] W.J. Takei, D.E. Cox, G. Shirane, Phys. Rev. 129 (1963) 2008.
[15] D. Scheerlinck, E. Legrand, Solid State Commun. 25 (1978) 181.

[16] M. Bacmann, J.-L. Soubeyroux, R. Barrett, D. Fruchart, R. Zach, S. Niziol, R. Fruchart, J. Magn. Magn. Mater. 134 (1994) 59.
[17] S. Fujii, S. Ishida, S. Asano, J. Phys. F Met. Phys. 18 (1988) 971.
[18] A. Koumina, M. Bacmann, D. Fruchart, J.L. Soubeyroux, P. Wolfers, J. Tobola, S. Kaprzyk, S. Niziol, M. Mesnaoui, R. Zach, Ann. Chim. Sci. Mater. 23 (1998) 177.
[19] J. Tobola, M. Bacmann, D. Fruchart, S. Kaprzyk, A. Koumina, S. Niziol, J.L. Soubeyroux, P. Wolfers, R. Zach, J. Magn. Magn. Mater. 157/158 (1996) 708.
[20] H. Fujii, T. Kabe, T. Kamigaichi, T. Okamoto, J. Phys. Soc. Jpn. 43 (1977) 41.
[21] B. Malaman, G. Le Caër, P. Delcroix, D. Fruchart, M. Bacmann, R. Fruchart, J. Magn. Magn. Mater. 8 (1996) 8653.